

Survival probability of large rapidity gaps in the QCD and N=4 SYM motivated model.

E. Gotsman^{a*}, E. Levin^{a,b†} and U. Maor^{a‡}

a) Department of Particle Physics, School of Physics and Astronomy, Raymond and Beverly Sackler Faculty of Exact Science, Tel Aviv University, Tel Aviv, 69978, Israel

b) Departamento de Física, Universidad Técnica Federico Santa María, Avda. España 1680, Casilla 110-V, Valparaiso, Chile

ABSTRACT: In this paper we present a self consistent theoretical approach for the calculation of the Survival Probability for central dijet production . These calculations are performed in a model of high energy soft interactions based on two ingredients:(i) the results of N=4 SYM, which at the moment is the only theory that is able to deal with a large coupling constant; and (ii) the required matching with high energy QCD. Assuming, in accordance with these prerequisites, that soft Pomeron intercept is rather large and the slope of the Pomeron trajectory is equal to zero, we derive analytical formulae that sum both enhanced and semi-enhanced diagrams for elastic and diffractive amplitudes. Using parameters obtained from a fit to the available experimental data, we calculate the Survival Probability for central dijet production at energies accessible at the LHC. The results presented here which include the contribution of semi-enhanced and net diagrams, are considerably larger than our previous estimates.

KEYWORDS: Soft Pomeron, BFKL Pomeron, Survival Probability, N=4 SYM.

PACS: 13.85.-t, 13.85.Hd, 11.55.-m, 11.55.Bq

*Email: gotsman@post.tau.ac.il.

†Email: leving@post.tau.ac.il

‡Email: maor@post.tau.ac.il.

1. Introduction	1
2. The main formulae: Good-Walker mechanism	3
3. Enhanced diagrams	3
4. Enhanced diagrams and semi-enhanced diagrams as a perturbation	5
5. Net diagrams.	6
6. Net and enhanced diagrams.	7
7. Numerical estimates and prediction for the LHC	8
8. Conclusions	9

1. Introduction

The original evaluation of the survival probability for a large rapidity gap (SPLRG) was made by Bjorken [1](see also Ref. [2]), in a one channel formalism, where the elastic amplitude was assumed to have a Gaussian shape in impact parameter space. This enabled him to obtain a closed analytic expression for $\langle |S^2| \rangle$, the SPLRG.

We [3] extended Bjorken's treatment to five different models, all of which reproduce the measured total cross sections at energies upto and including $\sqrt{s} = 1.8$ TeV. However, the values obtain from these models for $\langle |S^2| \rangle$ differed greatly, e.g. for the Tevatron energy they predicted values between 9.6 and 32.6%. Indicating that using parameters determined only from the elastic amplitude, was insufficient to determine $\langle |S^2| \rangle$ uniquely.

We then broadened our approach to a two channel Good-Walker description, which included elastic as well as diffractive channels [4]. This was called for, as the experimental data from the Tevatron [5] indicated that the diffractive channels were important and should not be neglected, $\frac{\sigma_{sd} + \sigma_{dd}}{\sigma_{elast}} \approx 0.85$. Including the

diffractive channels necessitated including also the triple Pomeron coupling, which plays a crucial role in determining $\langle |S^2| \rangle$.

The difficulty inherent in including the diffractive channels (i.e. $3\mathbb{P}$ coupling), is that one has to sum over all orders (loops) of these interactions, and there is no rigorous method for evaluating the so called enhanced and semi-enhanced (Pomeron) diagrams.

To make the problem tractable, we have in two previous papers (see Refs. [6, 7]) constructed a model of soft interactions at high energies based on the postulates that stem from N=4 SYM and QCD. The model includes the following features:

1. It is built using Pomeron and Reggeons as the main ingredients as follows from N=4 SYM(see Refs. [8–12]);
2. The intercept of the Pomeron should be rather large. In N=4 SYM [8, 13] we expect $\Delta_{\mathbb{P}} = \alpha_{\mathbb{P}}(0) - 1 = 1 - 2/\sqrt{\lambda} \approx 0.11 \sim 0.33$, based on estimates of $\lambda = 5 \sim 9$ derived from the early LHC measurements from the cross section of multiparticle production as well as from DIS at HERA [14].
3. As follows from N=4 SYM, the slope of the Pomeron $\alpha'_{\mathbb{P}}(0) = 0$, this is compatible with our fits to the cross section data in the ISR-Tevatron energy range [6, 7].
4. A large contribution to the cross section comes from processes of diffraction dissociation, as in N=4 SYM at large λ only these processes contribute to the scattering amplitude. In other words, in this model the Good-Walker mechanism [15] is the main source of diffractive production;
5. The Pomeron self-interaction should be small (of the order of $2/\sqrt{\lambda}$ in N=4 SYM), and much smaller than the vertex of interaction of the Pomeron with a hadron, which is of the order of λ ;
6. The last condition is not a prerequisite of N=4 SYM, but follows from the requirement of the natural matching with perturbative QCD, where the only vertex that contributes is the triple Pomeron vertex [16]. This ingredient differentiates our model from other models on the market (see Refs. [17, 18]);

In this paper we apply the theoretical approach that was developed to calculate the value for SPLRG processes at the LHC. This problem has been a subject of much discussion [6, 17] since our estimates first given in Ref. [6], suggested a small value of the survival probability for central Higgs boson production, in disagreement with the estimates of the Durham group [17]. In Ref. [6] we only included the enhanced Pomeron diagrams. In this paper we present our estimates for the full set of the diagrams. We discuss the important topic : the derivation of formulae for SPLRG processes originating from three sources: the Good-Walker mechanism, semi-enhanced diagrams and enhanced diagrams for the Pomeron interaction. We discuss this derivation in the first three sections, while the fourth section is devoted to numerical estimates.

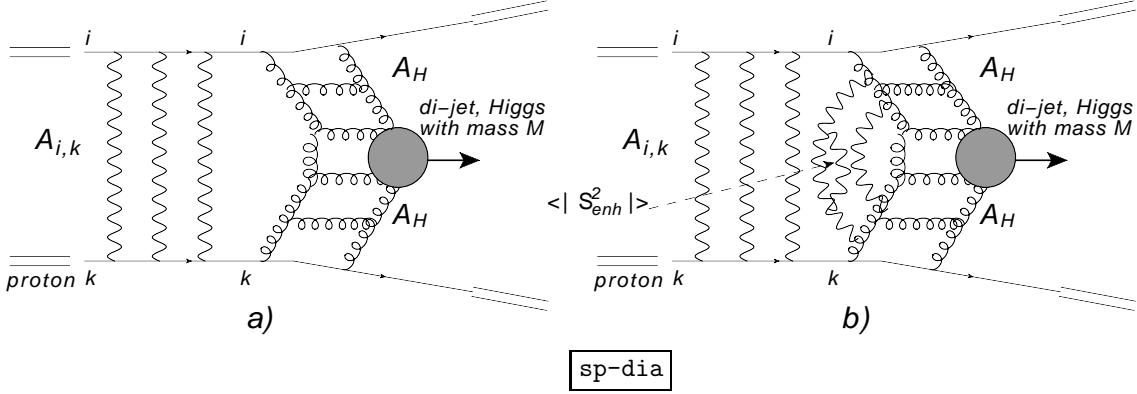


Figure 1: Survival probability for exclusive central diffractive production of the Higgs boson. Fig. 1-a shows the contribution to the survival probability in the G-W mechanism, while Fig. 1-b illustrates the origin of the additional factor $\langle |S_{enh}^2| \rangle$.

2. The main formulae: Good-Walker mechanism

The calculation of the survival probability for the hard processes is a choice example that shows that the cross section of the hard processes cannot be calculated, except for some special cases (total DIS cross section, inclusive cross sections), without a substantial knowledge of the ‘soft’ physics. The general formula for the Good-Walker mechanism (sum of the non-enhanced Pomeron diagrams) and for the sum of enhanced diagrams has the form

$$\langle |S^2| \rangle = \frac{\int d^2 b \left\{ \sum_{i,k} \langle p|i \rangle^2 \langle p|k \rangle^2 e^{-\frac{1}{2}\Omega_{i,k}(s,b)} S_{i,k}^H(b) \right\}^2}{\int d^2 b \left\{ \sum_{i,k} \langle p|i \rangle^2 \langle p|k \rangle^2 \int d^2 b' A_H^i(s,b) A_H^k(s, \vec{b} - \vec{b}') \right\}^2}, \quad (2.1) \quad \boxed{\text{SP}}$$

where, $\langle p|i \rangle$ is equal to $\langle \Psi_{proton} | \Psi_i \rangle$ and, therefore, $\langle p|1 \rangle = \alpha$ and $\langle p|2 \rangle = \beta$, $\alpha^2 + \beta^2 = 1$. Our notation as well as the derivation of Eq. (2.1) can be found in Ref. [19].

The factors $\exp[-\Omega_{i,k}/2]$ are responsible for the Good-Walker mechanism contribution for the survival probability, while the factors $S_{i,k}^H(b)$ account for an additional suppression due to a structure of the $\Omega_{i,k}$. In Fig. 2 we illustrate examples of the different contributions in $S_{i,k}^H$. Fig. 1, which is taken from our paper [6] shows that $S_{i,k}^H$ depends critically on both the hard and the soft amplitude. Our main goal is to find this dependence and calculate $S_{i,k}^H$. The parametrization of the hard amplitude $A_H^i(s, b_i)$ has been discussed in Ref. [6], and we refer the reader to this paper for details.

3. Enhanced diagrams

The calculation of the sum of the enhanced diagrams has been treated in detail in our previous papers [6, 7] and so we will not repeat the discussion here.

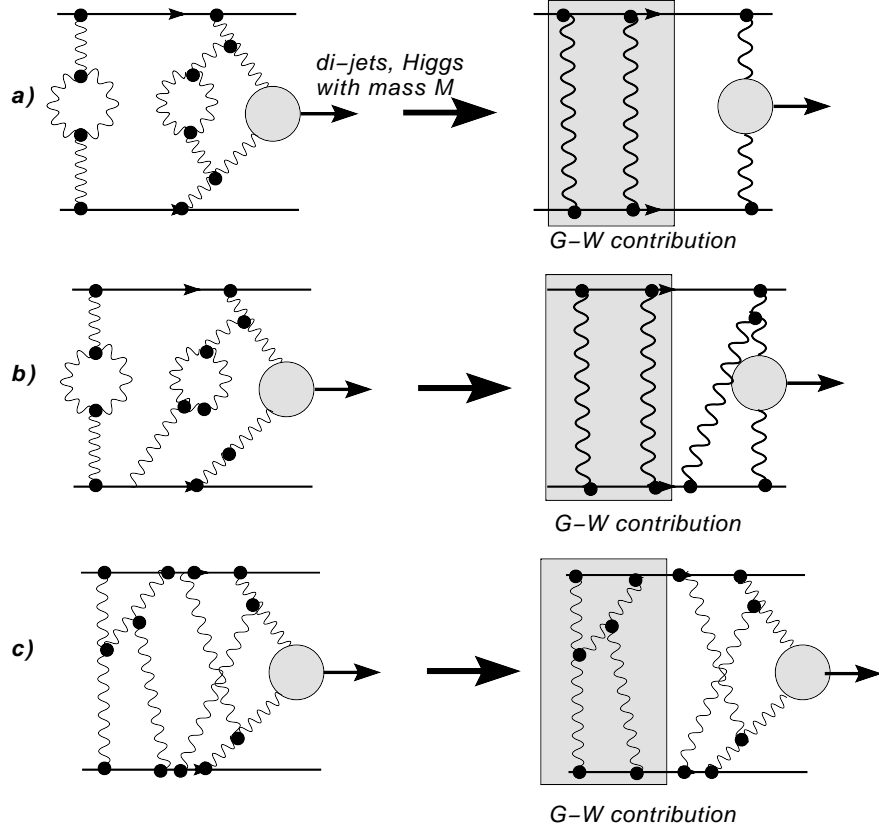


Figure 2: The set of diagrams that is selected and summed for the calculation of the survival probability for diffractive Higgs production. Fig. ^{spn}2-a shows the diagrams in G-W + enhanced diagrams approach, in Fig. ^{spn}2-b the same approach is shown, however, to calculate the value of the survival probability we add the first semi-enhanced diagram. The approach for $\tilde{g}_i T(Y) \approx 1$ but $\Delta_P T(Y) \ll 1$ (net diagrams) is shown in Fig. ^{spn}2-c.

spn

In the case of summing the enhanced diagrams the damping factors $S_{i,k}^H(b; b_1 b_2)$ have a simple structure

$$S_{i,k}^H(b; b_1 b_2) = \langle | S_{enh}(Y) | \rangle A_H^i(s, b_1) A_H^k(s, b_2), \quad (3.1) \quad \text{SPED1}$$

where $\langle | S_{enh}(Y) | \rangle$ depends only on energy (total rapidity $Y = \ln(s/s_0)$) and it can be considered to be a common factor. Although, this factor appears in Ref. [6], for completeness of the presentation it is given below.

$$\langle | S_{enh}^2(Y) | \rangle = \quad (3.2)$$

$$= S(\mathcal{T}(Y)) - 2 e^{-\Delta_P(Y-y_h)/2} S1(\mathcal{T}(Y)) + e^{-2\Delta_P(Y-y_h)/2} S2(\mathcal{T}(Y));$$

$$S(T) = \frac{1}{T^3} \left\{ -T + (1+T) e^{\frac{1}{T}} \Gamma\left(0, \frac{1}{T}\right) \right\}; \quad (3.3)$$

$$S1(T) = \frac{1}{T^3} \left\{ -T(1+T) + (1+2T) e^{\frac{1}{T}} \Gamma\left(0, \frac{1}{T}\right) \right\}; \quad (3.4)$$

$$S2(T) = \frac{1}{T^3} \left\{ T \left[(T-1)^2 - 2 \right] + (1+3T) e^{\frac{1}{T}} \Gamma\left(0, \frac{1}{T}\right) \right\}, \quad (3.5)$$

where

$$\mathcal{T}(Y) = \gamma \left(e^{\Delta_P(Y-Y')} - 1 \right) \left(e^{\Delta_P Y'} - 1 \right). \quad (3.6) \quad \boxed{\text{TT}}$$

$\Gamma(0, 1/T)$ is the incomplete gamma function (see formulae 8.35 in Ref. [20]).

4. Enhanced diagrams and semi-enhanced diagrams as a perturbation

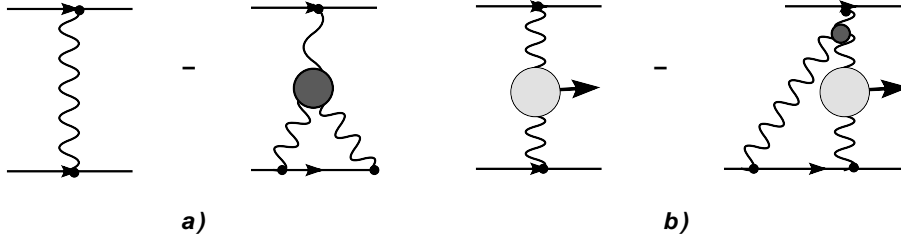


Figure 3: The set of diagrams in terms of the exact Pomeron and exact vertices that we include in our perturbative approach for the summation of semi-enhanced diagrams. Fig. ^{seen}3-a gives contribution to $\Omega_{i,k}$ (see section 2.3) while Fig. ^{seen}3-b shows the changes in $S_{i,k}^H$. seen

As has been discussed in our approach based on the summation of the enhanced diagrams (see Ref. [6]) the contribution of the semi-enhanced diagrams to the value of the survival probability has been neglected. The first correction due to such a contribution is shown in Fig. ^{spn}2-b (compare with Fig. ^{spn}2-a). The expression for this correction has the form (see Fig. ^{seen}3-b)

$$\langle | S_{i,k}^H(\text{Fig. } \text{seen} \text{ 3-b}; Y, b) | \rangle = \int d^2 b_1 \left\{ \langle | S_{enh}^2(Y) | \rangle A_i^H(Y, b_1) A_i^H(Y, \vec{b} - \vec{b}_1) \right. \quad (4.1)$$

$$- 2 \int^Y dy_1 \int^{y_1} dy_2 \int^{y_2} dy_3 G(Y - y_1) \Gamma(y_1, y_2, y_3) G(y_2 - 0) \langle | S_{enh}^2(y_2) | \rangle \\ \times A_i^H(Y, \vec{b} - \vec{b}_1) \int d^2 b' A_k^H(Y, b') \tilde{g}_k(\vec{b}_1 - \vec{b}') \left. \right\}. \quad (4.2)$$

The coefficient 2 stems from two diagrams where the exact Pomeron is attached to upper and lower proton in Fig. ^{seen}3-b. $G(Y)$ is the exact Green's function of the Pomeron and is given by

$$G(Y) = 1 - \exp\left(-\frac{1}{T(Y)}\right) \frac{1}{T(Y)} \Gamma\left(0, \frac{1}{T(Y)}\right) \quad (4.3) \quad \boxed{\text{G}}$$

with

$$T(Y) = \gamma e^{\Delta_P Y}. \quad (4.4) \quad \boxed{\text{ES11}}$$

$\Gamma(y_1, y_2, y_3)$ is the exact vertex that has been discussed in section 3.4 of Ref. [7]. It is equal to

$$\Gamma(y_1, y_2, y_3) = \quad (4.5)$$

$$= \frac{\Delta_P}{4} \frac{1}{T(y_1 - y_2) - T(y_1 - y_3)} \{ \Gamma_1(2T(y_1 - y_2)) - \Gamma_1(2T(y_1 - y_3)) \} \quad (4.6)$$

$$\text{with } \Gamma_1(T) = (1/T^3) \times \{ T(1+T) - \exp(-1/T) (1+2T) \Gamma(0, 1/T) \}. \quad (4.7)$$

To calculate the survival probability we need to introduce the additional change in $\Omega_{i,k}$ in Eq. (2.1) (see for example Ref. [21] for detailed arguments). The resulting $\Omega_{i,k}$ has the form (see Fig. ^{seen}3-a)

$$\Omega_{i,k}(Y, b) = \int d^2 b_1 \left\{ G(Y) \tilde{g}_i(b_1) \tilde{g}_i(\vec{b} - \vec{b}_1) \right. \quad (4.8)$$

$$- 2 \int^Y dy_1 \int^{y_1} dy_2 \int^{y_1} dy_3 G(Y - y_1) \Gamma(y_1, y_2, y_3) G(y_2 - 0) G(y_3 - 0) \\ \times \tilde{g}_i(\vec{b} - \vec{b}_1) \int d^2 b' \tilde{g}_k(b') \tilde{g}_k(\vec{b}_1 - \vec{b}') \left. \right\}. \quad (4.9)$$

5. Net diagrams.

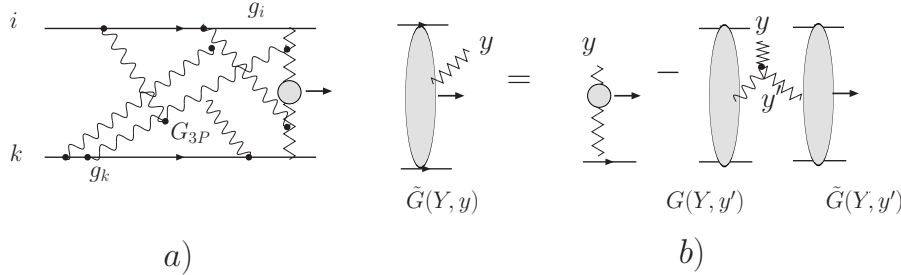


Figure 4: The set of diagrams (see Fig. ^{eqnd}4-a) for $S_{i,k}^H$ in the approximation where $\tilde{g}_i Y(Y) \approx 1$ while $\Delta T(Y) \ll 1$ (net diagrams) and the graphic form of the equation for $S_{i,k}^H \equiv \tilde{G}_{i,k}$. Zigzag line denotes the hard Pomerons. $\boxed{\text{eqnd}}$

In this section we discuss the survival probability in the approximation where $\tilde{g}_i T(Y) \approx 1$ while $\Delta_P T(Y) \ll 1$. In this approximation we need to sum a ‘net’ system of the diagrams, an example of which is shown in Fig. ^{eqnd}4-a. To find $S_{i,k}^H$ we introduce the function $\tilde{G}_k(Y; y)$ for which we can write the equation (see Fig. ^{eqnd}4-b)

$$\tilde{G}(Y, y) = A_k^H(b_1) - \Delta \int^y dy' G(Y, y') \tilde{G}(Y, y'). \quad (5.1) \quad \boxed{\text{SPND1}}$$

Eq. ^{SPND1}(5.1) can be rewritten in the differential form as

$$\frac{d\tilde{G}(Y, y)}{dy} = - \Delta G(Y, y') \tilde{G}(Y, y'). \quad (5.2) \quad \boxed{\text{SPND2}}$$

The solution to Eq. (5.2) is

$$\begin{aligned}\tilde{G}(Y, y) &= A_k^H(b_1) \exp \left\{ - \int_0^y \Delta G(Y, y') dy' \right\} \\ &= A_k^H(b_1) \frac{1}{1 + \tilde{g}_i(b_2) T(Y) + \tilde{g}_k(b_1) T(y)}.\end{aligned}\quad (5.3)$$

$S_{i,k}^H$ can be expressed with the aid of the functions \tilde{G} in the following way:

$$\begin{aligned}S^H(Y, b) &= \int d^2 b_1 A_i^H(\vec{b} - \vec{b}_1) A_k^H(b_1) \times \frac{1}{\left(1 + (G_{3P}/\gamma) \left(\tilde{g}_k(\vec{b} - \vec{b}_1) T(Y) + \tilde{g}_i(b_1) T(Y/2 - y_h/2)\right)\right)} \\ &\times \frac{1}{\left(1 + (G_{3P}/\gamma) \left(\tilde{g}_i(\vec{b} - \vec{b}_1) T(Y) + \tilde{g}_k(b_1) T(Y/2 + y_h/2)\right)\right)},\end{aligned}\quad (5.4)$$

where $y_h = \ln(M^2/s_0)$ and M denotes the mass of the produced system (dijets, Higgs boson etc.) and $s_0 = 1 \text{ GeV}^2$.

Finally to calculate the survival probability we require $\Omega_{i,k}$ which was derived in Ref. [7]

$$\Omega_{i,k} = \frac{1}{2} \int d^2 b' \frac{\tilde{g}_i(\vec{b}') \tilde{g}_k(\vec{b} - \vec{b}') (1/\gamma) T(Y)}{1 + (G_{3P}/\gamma) T(Y) [\tilde{g}_i(\vec{b}') + \tilde{g}_k(\vec{b} - \vec{b}')]}.\quad (5.5) \quad \boxed{\text{SPND5}}$$

6. Net and enhanced diagrams.

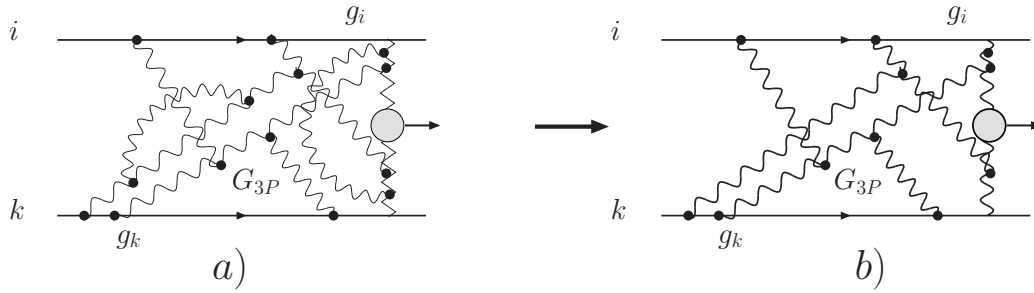


Figure 5: The net and enhanced diagrams (Fig. 5-a) and the set of diagrams with the exact Green's function of Pomeron and exact vertices (Fig. 5-b). Zigzag line denotes the hard amplitudes. $\boxed{\text{eqnden}}$

In the spirit of our approach we can generalize Eq. (5.4) and Eq. (5.5) taking into account the enhanced diagrams. As we have discussed, we need to replace $T(Y)$ by $G(T(Y))$ in these equations (see Fig. 5-a and Fig. 5-b) and to multiply Eq. (5.4) by $\langle |S_{enh}^2(Y)| \rangle$. This factor is responsible for summing the diagrams where the Pomeron lines are attached to the hard amplitude ('hard Pomeron') (see Fig. 5-a). $\boxed{\text{eqnden}}$

7. Numerical estimates and prediction for the LHC

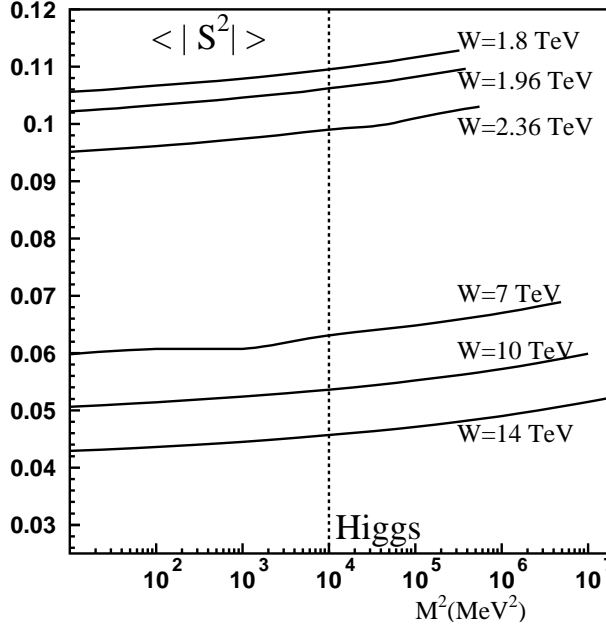


Figure 6: The estimates for the value of SP for dijets with mass M . The dotted line corresponds to the Higgs boson production with $M_{higgs} = 100 \text{ GeV}$. We estimate a $60 \div 70\%$ margin of error in our results. sp

Using Eq. [\(5.4\)](#) and Eq. [\(5.5\)](#) we have calculated the survival probability as a function of produced di-jets mass at c.m. energies of interest. We estimate the margin of errors of our results to range from 60% at $W=2 \text{ TeV}$ to 70% at $W=14 \text{ TeV}$. The central values obtained are shown in Fig. [6](#). sp

The main feature of our SP results is that their values are considerably larger than the values obtained in our previous studies [7]. Our current estimates are compatible with the CDF Tevatron data [22] as well as with the theoretical estimates [23, 24].

Our calculations presented in Ref. [6] only summed over the enhanced diagrams, while our present calculations sum over the complete set of enhanced, semi-enhanced and net diagrams. Comparing the fitted values of our parameters in the two studies we note that our present fitted values of γ and G_{3P} are much smaller than those obtained in Ref. [6]. Consequently, the screening initiated by the enhanced diagrams with the present parameters is much smaller than the screening caused by the same diagrams in our previous study. On the other hand, in our both papers we found out that (i) the main source of the small values of the SP is the enhanced diagrams; and (ii) the enhanced diagrams are the only cause for the dependence of the SP value on the mass of produced di-jets. Therefore, the rather large value of SP and its mild dependence of the mass of produced di-jets have the same origin: the small values of G_{3P} .

8. Conclusions

Fig. ^{SP} shows our estimates and predictions for the value of the SP. These values are the results of our theoretically self consistent approach that has been discussed in Refs. [6, 7]. We predict the value of the SP for Higgs production ($M_{Higgs} = 100 \text{ GeV}$) of about 3 – 5% for the LHC range of energies. These values are much larger our previous estimates, for a model in which only enhanced diagrams were taken into account [6]. Our main conclusions are that the value of the SP, as well as its mass dependence are very sensitive to both the particular form adopted for the Pomeron interaction, and to the values of the fitted parameters that determine the strength of the contribution of the enhanced diagrams.

The lesson from our present study is straight forward and discouraging to an extent, since we need a thorough knowledge of the theory of interacting Pomerons to guarantee the value of the SP. On the other hand, the model we constructed incorporates the main features of two compelling theoretical approaches: N=4 SYM and perturbative QCD.

We conclude that our theoretical knowledge of Pomeron interactions, as well as the set of available experimental data, are not sufficient to determine the strength of the Pomeron interaction with adequate accuracy, so as to provide precise estimates for the SP.

References

- [BJ] [1] J.D. Bjorken, Phys.Rev. D47 (1993) 101-113.
- [DOK] [2] Yuri L. Dokshitzer, Valery A. Khoze, T. Sjostrand, Phys.Lett. B274 (1992) 116-121.
- [GLM1] [3] E. Gotsman, E.M. Levin, U. Maor, Phys.Lett. B309 (1993) 199-204, e-Print: hep-ph/9302248; Phys. Lett. **B438** (1998) 229-234, [hep-ph/9804404]; Phys. Rev. **D60** (1999) 094011, [hep-ph/9902294]; E. Gotsman, E. Levin, U. Maor *et al.*, [hep-ph/0511060]; E. Gotsman, H. Kowalski, E. Levin *et al.*, Eur. Phys. J. **C47** (2006) 655-669. [hep-ph/0512254].
- [GLM2] [4] E. Gotsman, E. Levin, U. Maor, [arXiv:0708.1506 [hep-ph]]; Braz. J. Phys. **38** (2008) 431-436. [arXiv:0805.0418 [hep-ph]]; Phys. Lett. **B452** (1999) 387-394. [hep-ph/9901416]; E. Gotsman, A. Kormilitzin, E. Levin *et al.*, Eur. Phys. J. **C52** (2007) 295-304. [hep-ph/0702053];
- [atron] [5] CDF Collaboration (F. Abe ety al.), Phys.Rev. D50 (1994) 5535-5549; E710 Collaboration (Norman A. Amos et al.), Phys.Lett. B301 (1993) 313-316
- [GLMM] [6] E. Gotsman, E. Levin, U. Maor and J. S. Miller, Eur. Phys. J. **C57** (2008) 689-709. [arXiv:0805.2799 [hep-ph]].
- [GLMLA] [7] E. Gotsman, E. Levin, U. Maor, Eur. Phys. J. **C71** (2011) 1553, [arXiv:1010.5323 [hep-ph]].
- [BST] [8] R. C. Brower, J. Polchinski, M. J. Strassler and C. I. Tan, JHEP **0712** (2007) 005 [arXiv:hep-th/0603115]; R. C. Brower, M. J. Strassler and C. I. Tan, JHEP **0903** (2009) 092 [arXiv:0710.4378 [hep-th]]; JHEP **0903** (2009) 050. [arXiv:0707.2408 [hep-th]].
- [HIM] [9] Y. Hatta, E. Iancu and A. H. Mueller, JHEP **0801** (2008) 026 [arXiv:0710.2148 [hep-th]].
- [COCO] [10] L. Cornalba and M. S. Costa, Phys. Rev. **D 78**, (2008) 09010, arXiv:0804.1562 [hep-ph]; L. Cornalba, M. S. Costa and J. Penedones, JHEP **0806** (2008) 048 [arXiv:0801.3002 [hep-th]].

- [BEP] [11] B. Pire, C. Roiesnel, L. Szymanowski and S. Wallon, Phys. Lett. B **670**, 84 (2008) [arXiv:0805.4346 [hep-ph]].
- [LMKS] [12] E. Levin, J. Miller, B. Z. Kopeliovich and I. Schmidt, JHEP **0902**, 048 (2009) [arXiv:0811.3586 [hep-ph]].
- [BFL4] [13] A. V. Kotikov, L. N. Lipatov, A. I. Onishchenko and V. N. Velizhanin, Phys. Lett. B **595** (2004) 521 [Erratum-ibid. B **632** (2006) 754] [arXiv:hep-th/0404092]; A. V. Kotikov and L. N. Lipatov, Nucl. Phys. B **661** (2003) 19 [Erratum-ibid. B **685** (2004) 405] [arXiv:hep-ph/0208220]; A. V. Kotikov and L. N. Lipatov, Nucl. Phys. B **582** (2000) 19 [arXiv:hep-ph/0004008]. A. V. Kotikov, L. N. Lipatov and V. N. Velizhanin, Phys. Lett. B **557** (2003) 114 [arXiv:hep-ph/0301021]; J. R. Andersen and A. Sabio Vera, Nucl. Phys. B **699** (2004) 90 [arXiv:hep-th/0406009];
- [LEPO] [14] E. Levin and I. Potashnikova, JHEP **1008** (2010) 112; [arXiv:1007.0306 [hep-ph]]; R. C. Brower, M. Djuric, I. Sarcevic, C. -ITan, JHEP **1011** (2010) 051, [arXiv:1007.2259 [hep-ph]].
- [GW] [15] M. L. Good and W. D. Walker, Phys. Rev. **120** (1960) 1857.
- [BART] [16] J. Bartels, M. Braun and G. P. Vacca, Eur. Phys. J. **C40** (2005) 419 [arXiv:hep-ph/0412218]. J. Bartels and C. Ewerz, JHEP **9909** 026 (1999) [arXiv:hep-ph/9908454]. J. Bartels and M. Wusthoff, Z. Phys. **C6**, (1995) 157. A. H. Mueller and B. Patel, Nucl. Phys. **B425** (1994) 471 [arXiv:hep-ph/9403256]. J. Bartels, Z. Phys. **C60** (1993) 471.
- [KMRS] [17] M. G. Ryskin, A. D. Martin, V. A. Khoze *et al.*, J. Phys. G **G36** (2009) 093001 [arXiv:0907.1374 [hep-ph]]; Eur. Phys. J. **C60** (2009) 265-272. [arXiv:0812.2413 [hep-ph]]; Eur. Phys. J. **C60** (2009) 249-264. [arXiv:0812.2407 [hep-ph]]; AIP Conf. Proc. **1105** (2009) 252-257. [arXiv:0811.1481 [hep-ph]]; “*Soft Diffraction at the LHC*,” arXiv:0810.3324 [hep-ph]; “*Rapidity gap survival probability and total cross sections*,” arXiv:0810.3560 [hep-ph]; Eur. Phys. J. **C54** (2008) 199 [arXiv:0710.2494 [hep-ph]].
- [OS] [18] S. Ostapchenko, Phys. Rev. D **81** (2010) 114028 [arXiv:1003.0196 [hep-ph]]; Phys. Rev. D **77** (2008) 034009 [arXiv:hep-ph/0612175]; Phys. Lett. B **636** (2006) 40 [arXiv:hep-ph/0602139].
- [2CH] [19] E. Gotsman, E. Levin and U. Maor, Phys. Lett. **B452** (1999) 387; **B309** (1993) 199; Phys. Rev. **D49** (1994) R4321.
- [RY] [20] I. Gradstein and I. Ryzhik, “*Tables of Series, Products, and Integrals*”, Verlag MIR, Moskau, 1981.
- [BORY] [21] K. G. Boreskov, A. B. Kaidalov, V. A. Khoze, A. D. Martin and M. G. Ryskin, Eur. Phys. J. **C44** (2005) 523 [arXiv:hep-ph/0506211].
- [CDF] [22] T. Aaltonen *et al.* [CDF Collaboration], Phys. Rev. **D77** (2008) 052004. [arXiv:0712.0604 [hep-ex]].
- [MRCDF] [23] V. A. Khoze, A. D. Martin, M. G. Ryskin, Frascati Phys. Ser. **44** (2007) 147-160, [arXiv:0705.2314 [hep-ph]].
- [ROYON] [24] C. Royon, R. Staszewski, A. Dechambre, O. Kepka, PoS **DIS2010** (2010) 087, [arXiv:1008.0255 [hep-ph]]; O. Kepka, C. Royon, Phys. Rev. **D76** (2007) 034012, [arXiv:0704.1956 [hep-ph]].